

FIELD-ALIGNED CURRENT DYNAMICS DURING TWO SUBSTORMS OF SUMMER AND WINTER TYPES AND MODEL FOR THE ELECTRIC CIRCUIT OF THE MAGNETOSPHERE-IONOSPHERE SYSTEM OF TWO HEMISPHERES

V.M. Mishin, V.V. Mishin, M.A. Kurikalova, Yu.A. Karavaev, and O.I. Bergardt (*Institute of Solar-Terrestrial Physics of Siberian Branch of Russian Academy of Sciences*)

Abstract. Based on the time series from maps of field-aligned current (FAC) distribution in the ionosphere, we developed an empirical scenario for the substorm expansion phase (EP) in two hemispheres. Its peculiarities are:

1) We took into account mesoscale cells with the FAC density local maximum inside each Iijima and Potemra (I-P) Region, which augmented the spatial resolution two- or threefold.

2) We described two types of the FAC distribution in the nightside polar ionosphere, observed during the substorm EP in the winter and summer hemisphere, respectively. These two types start simultaneously in two hemispheres, but in different MLT-sectors of the nightside Region 1 that are separated by ~6 MLT.

3) We revealed that the **global** magnetosphere-ionosphere (M-I) feedback instability in the summer hemisphere premidnight sector serves as an initiator and organizer of the global EP.

4) We designed a schematic model for the electric circuit of the disturbed nightside M-I system. The model describes the above distributions of FAC, ionospheric currents, and partial ring current. We note the contribution of the ring current to the M-I feedback instability evolution.

1. Introduction

The current scenarios for magnetospheric substorms are based on satellite measurement data, as well as on the ground-based measurements [e.g., *McPherron et al.*, 1973; *Baker et al.*, 1996; *Lui et al.*, 1996; *Angelopoulos et al.*, 2008; *Akasofu*, 2015]. They address a typical substorm as a global phenomenon, where signatures of the hemisphere asymmetry are established facts, and the asymmetry manifestations are significant [e.g., *Ostgaard et al.*, 2011; *Reistad et al.*, 2014; *Laundal and Ostgaard*, 2009; *Knipp et al.*, 1993; *Lu et al.*, 2011]. However, the scope of the accumulated database from the ground-based measurements in the Southern Hemisphere is tenfold smaller, than that for the Northern Hemisphere. Thereupon, we note that the known manifestations of the typical substorm asymmetry do not affect the fundamental signatures of the typical substorm expansion phase (EP). On the other hand, there is individual evidence that the substorm current systems differ dramatically in the Earth's two hemispheres (at least, near the EP maximum times) [*Mishin et al.*, 2015a]. It is the summer hemisphere, where EP manifests itself like a spontaneous manifold increase in the downward field-aligned current (FAC) in the R1 premidnight sector of the summer hemisphere. Hereinafter, we denote this site as "R1- cell." The impulse lasts for ~10 minutes. In contrast, in the winter hemisphere, in this sector, one observes the FAC collapse, although, in the adjacent R1 postmidnight sector, one simultaneously observes the EP signatures. The above two sectors constitute the most active EP interval ~(06-18) MLT [*Kissinger et al.*, 2012]. The centers of these two sectors of the winter hemisphere are separated by 6 MLT. The FAC directions in the winter hemisphere two sectors are opposite. In the summer hemisphere premidnight sector, one observes the signatures of the M-I feedback instability that are absent in the winter hemisphere. Thus, according to the empirical data from *Mishin et al.* [2015a], the substorm in two hemispheres is initiated and driven from the above R1- cell of the summer hemisphere.

We developed this scenario from the data on the pair of substorms observed in the Northern Hemisphere, one during the summer season, whereas the other was observed during winter season. *Mishin et al.* [2015c, Associated paper] find out the applicability of this scenario to substorms of the equinox season. This paper is the continuation of this study. We use the designations, conclusions, and figures from the Associated paper referring to the latter as "As-paper." The figures are denoted as "NAs Fig.", where N is the Figure number. We use the quantitative data from the As-paper to design the schematic diagram for the EP electric circuit. The diagram combines the pair of the winter- and summer-type EP events denoted as «Events 1 and 2», respectively, in the As-paper. Here, "winter" and "summer" do not denote the local season, but rather the substorm EP content described in the As-paper. Fig. 2 in the As-paper provides the skeleton of the above schematic model. We need its description in the As-paper to understand the further text.

2. Model for the M-I system electric circuit during EPs of Events 1 and 2

2.1 To combine two EPs within a common schematic model for the substorm global EP, we chose Events 1 and 2 which are an amazing, but typical of the equinox, example. In this example, the EP regime changes fundamentally from the above "winter" to the above "summer" type for two hours, at transition from the (02-03) UT interval to (03-04) UT. Fig. 1 provides this combining model. The figure was obtained based on Fig. 2As that is the model skeleton (without numbers). The terms RN_{\pm} and rN_{\pm} specify the position of each cell in the polar regions of two hemispheres

(see additionally Fig. 1 As). Over each RN^\pm and rN^\pm cell in Fig. 1, we mark the normalized values of I'_{RN^\pm} , or I'_{rN^\pm} , FAC intensities (in kA). Here, $I'_{RN^\pm} = k \cdot I_{RN^\pm}$, where $k = I_{R1^\pm}/I_{rN^\pm}$, i.e. the "k" coefficient is the ratio of the FAC intensity in the input cell from generator G into the M-I system of the Northern Hemisphere to the FAC intensity in the input cell of the Southern Hemisphere. The I_{R1^\pm} and I_{rN^\pm} values are the real values of the FAC intensity of FAC on the plots of Figs. 3 As and 4 As for the 0255 UT and 0335 UT, respectively. At these instants, one observes spontaneous maxima for two EPs of Events of 1 and 2, summer and winter types, respectively.

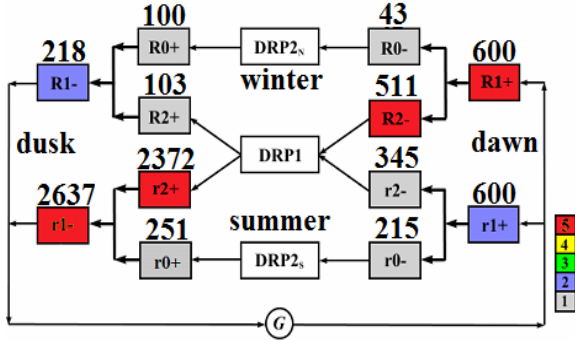


Figure 1. The scheme for the current electric circuit of the substorm expansion phase in the nightside hours. The upper half shows the summer hemisphere, the lower half present the winter one. It is shown the mutual location of RN^\pm cells, of the DRP1 partial ring current, and of DRP2 magnetospheric currents.

Over the cells, the normalized FAC intensity values are presented in kA. Inside the cells, also the FAC intensity estimates (points 1 through 5) are shown .

The normalization equalizes the input FAC values in the Northern and Southern Hemispheres. Fig. 1 also shows the FAC intensity estimates (in points) that are proportional to the FAC intensity numerical values. The point values are provided with the numbers (1 through 5) inside each cell (and in color in the colored version of the figures). The points were determined individually for each hemisphere.

Thus, the Fig. 1 model meets three necessary requirements to the model that describes two different EP phases: the winter type in any hemisphere, and the summer type in the opposite hemisphere. These requirements are: 1) belonging of both EP phases to the season common for two hemispheres: "November-February" or "May-August", or "equinox"; 2) two EP phases are to have comparable FAC intensity values at the inputs from the generator (the $I_{R1^\pm} \approx I_{r1^\pm}$ condition), or one should propose such a normalization technique that allows one to bypass the issue of comparable, or different values of the input FACs in two hemispheres; 3) both EP phases are to occur at the above FAC maximum instant physically common for them. The latter implies that, near the selected EP maximum instants, the FAC intensity increases manyfold within ~ 10 minutes, and reaches the FAC level that is higher than the initial level controlled by the boundary conditions. Under such circumstances, the FAC intensity values are mostly determined by the properties of the instability producing EP. The sufficiency degree of these requirements for the typical global EP model is determined by the percent of recurrence of substorms that possess the corresponding different EP types in two different hemispheres. So far, we have studied 4 substorm pairs with the summer-type EP in one hemisphere and the winter-type EP in the other. The recurrence is 100%.

2.2. M-I coupling and M-I feedback of two hemispheres during expansion phase

The model for the electric circuit in Fig. 1 is based on the description of its skeleton (Fig. 2As) and the FAC intensity variation plots (Fig. 3As). The upper (lower) half of Fig. 1 corresponds to the model winter- (summer-) type EP in the model Northern (Southern) Hemisphere. We note the I_{r1-} maximum (2372 kA) in the $r1-$ cell of the above summer hemisphere, and the I_{R1+} maximum (600 kA) in the $R1+$ cell of the winter (Northern) hemisphere. These two maxima are causally related. Indeed, tracing the flows of the FACs arriving in the above input cells of two hemispheres, one can see that a strong $r1-$ instability intensifies the FAC in the generator and in the $R1+$ cell, thereby producing the M-I coupling of two hemispheres. Further, however, we see the $I_{R2-} > I_{2+}$ inequality, which corresponds to the return of the FAC part from the Northern to the Southern Hemisphere. Thus, the formation of the electric circuit leads to the M-I coupling, as well as to the MI-feedback of two hemispheres.

2.3. Nightside FAC system collapse

The above $I_{R2-} > I_{2+}$ inequality, together with a small I_{R0+} value (100 kA), leads to the FAC intensity minimal for $R1$ ($I_{R1-} = 218$ kA). The full I_{R1+} FAC arriving from the generator into the winter hemisphere is not used in this hemisphere, but closes onto the generator through the DRP1 ring current and $r1-$ cell. Thus, despite the $I_{R1+} = I_{r1+}$ equality, the formation of the EP circuit presented in Fig. 1 leads to the $I_{R1-} < I_{R1+}$ inequality. There is no such a dawn>dusk asymmetry in the FAC intensity distribution within the nightside $R1$ and $R2$ in the statistical FAC model (e.g., *Potemra*, 1994). In contrast, such an asymmetry is a common EP property for three winter substorms that we chose randomly and addressed [*Mishin et al.*, 2015a, b]. We term this new phenomenon a "FAC collapse" in the dusk sector of the nightside $R1$ during EP in the winter hemisphere. *Murphy et al.* [2012], *Pellinen and Heikkila* [1978] noted something similar before. The above $I_{R1-} < I_{R1+}$ inequality is one of the causes for such a collapse. We note the other reason in Paragraph 2.5.

2.4. Role of the DRP1 ring current in producing the M-I current system of two hemispheres

Comparing the numerical values of $I_{R2-} = 511$ kA and $I_{R1-} = 2372$ kA shows a strong $I_{R2-} \gg I_{R1-}$ inequality. We observed such a strong inequality only in one case, but the sign and the value of the inequality $\sim (10^2 \div 10^3)$ kA persisted in all the addressed substorms. These inequalities provide a numerical estimate of the DRP1 partial ring current contribution to producing the M-I coupling of the common current system in two hemispheres.

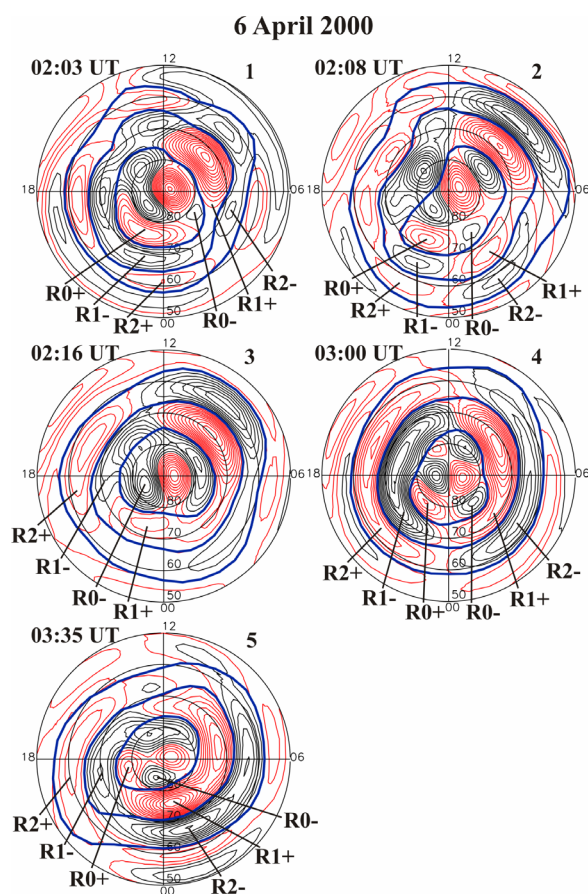


Figure 2. Examples of the FAC density distribution in the Northern Hemisphere polar ionosphere. Solid/dotted lines show the upward/downward FAC. In the MLT night half, the $R_{N\pm}$ symbols mark the centers of the mesoscale cells. On Maps 2 and 4, the downward and upward FACs in R1 are located symmetrically relative to midnight. On Map 1, one can see the dusk>dawn asymmetry (the upward FAC distribution is twisted counter-clockwise). Maps 3 and 5 provide the examples of the clockwise twisting.

local processes of the tail extension and dipolarization during substorms. Each of these processes produces a strong ($\sim 10^6$ A) X-current in the tail plasma sheet [Lui and Kamide, 2003]. We assume that this current density is inhomogeneous along the X-axis, and it is this that produces the X-current divergence, i.e., a FAC area extended on the X-axis along the inhomogeneity. The direction of such a FAC depends on two factors. The first factor is the tail extension, or dipolarization. The other factor is the X-current gradient direction in the inhomogeneity producing the twisted FAC area. Four combinations of these two factors are possible. They are the following: (1) "the tail extension and the above gradient Earthward", (2) "the tail extension and the above gradient off-Earth", (3) "the tail magnetic field dipolarization and the above gradient Earthward", (4) "the tail magnetic field dipolarization and the above gradient off-Earth." Combination 1 (2) produces the upward (downward) FAC in the ionosphere, where the tail X-current closes. Combination 3 (4) produces the downward (upward) FAC in the area, where it is implemented. Thus, the four combinations describe the clockwise and counter-clockwise twisting presented in Fig. 2, both at the tail local extension and at the tail local dipolarization.

2.5 Azimuthal twisting and untwisting of the FAC system

Fig. 2 shows the maps of different types of the FAC distribution in the addressed Events 1 and 2.

A special difference in this type FAC distribution from the expected FAC distribution in the Iijima and Potemra model is a signature for each type. In this model, the distribution of the nightside FAC density and intensity is approximately symmetrical relative to the meridian separating the downward and upward FACs. Due to the restricted paper scope, we describe the signatures for each type here referring only to R1, although similar signatures are also observed in R0 and R2. Fig. 2 presents the examples of these signatures in R1. They are the following.

Type 1, 0203 UT: one observes the dusk>dawn asymmetry in the distribution of the FAC density and intensity, and counter-clockwise twisting of the upward FAC distribution in the nightside R1.

Type 2, 0208 UT: there occurs an I-P-type FAC distribution in the nightside R1. One can see two weak cells of the substorm current wedge, without the dawn/dusk asymmetry and the corresponding twisting.

Type 3, 0216 UT: one can see the prevalence of the downward FAC in the premidnight and postmidnight sectors in the nightside R1 as a result of the FAC distribution clockwise twisting. The twisting leads to an upward FAC westward displacement in the R1 premidnight sector, which results here in the partial collapse (intensity decrease) of the upward FAC.

Type 4, 0300 UT: in the nightside R1 (and in R2), there was established a FAC distribution of a strong intensity and of the I-P model type without the dawn-dusk asymmetry at the EP peak.

Type 5, 0335 UT: signatures of clockwise twisting of the FAC distribution emerged again in the nightside R1.

Note that the term "twisting" does not assume the process in time, but the result of reconfiguration of the FAC spatial distribution. The physics of the "twisting" phenomena is yet to be studied. As a possible version, we note that similar phenomena may be created by

3. Summary

1. From the data on the 2000 April 6 two selected events, we calculated the maps for FAC density distribution in the polar ionosphere of the Northern Hemisphere. In each event, sufficient signatures of expansion phase were observed. In one of them, we describe the EP type termed "summer," and the one termed "winter" in the other event.

2. We propose a scenario for the global EP, where this substorm phase evolves simultaneously in the summer and winter hemispheres, but in different MLT sectors of the nightside R1 offered: the winter (summer) type EP is observed in the R1 postmidnight (premidnight) sector. These two sectors are within the \sim (18-06) MLT interval, and their centers are separated by \sim 6 MLT.

3. We substantiated the conclusion that the M-I feedback instability in the R1 premidnight sector of the summer hemisphere serves as an initiator and an organizer of the global EP.

4. In the winter hemisphere, a collapse (a decrease in the downward FAC intensity) of the R1 premidnight sector FAC system evolves simultaneously with the EP of the postmidnight sector. We describe the physics of this collapse within the model for the electric circuit of the common current system in the global EP M-I system.

5. We described the phenomena of spontaneous reconfiguration of the FAC density and intensity distribution in R1 and other Iijima and Potemra Regions. The reconfiguration is observed as a variation in the FAC density and intensity distributions in I-P Regions. These variations produce an expansion/compression of the downward FAC sector due to a compression/expansion of the upward FAC in the adjacent sector of the same Region. These phenomena are described in terms of azimuthal "twisting" of the FAC density spatial distribution in each I-P Region (clockwise or counter-clockwise).

6. We propose a conceptual model for twisting phenomena based on the supplemented model from *Lui and Kamide* [2003].

In general, we suggest an empirical scenario for the global EP involving principally new elements, as compared with the known substorm scenarios.

We introduced the new elements based on **combining the data on two hemispheres**, winter and summer, within a uniform model for the electric circuit of the M-I current system. Unlike such an approach, the known empirical substorm scenarios are primarily made on the database for the Northern Hemisphere. In this case, the strong asymmetry of two hemispheres - the key element of the proposed EP scenario - is not taken into account.

Acknowledgements. We thank the ISTP SB RAS MIT group members for stimulating discussions. The AE index was obtained from the World Data Center for Geomagnetism, Kyoto. We are grateful to PIs of the CANOPUS, INTERMAGNET, GIMA, MACCS, IMAGE projects and of magnetic networks in Arctic and the Antarctic (the Shafer Institute of Cosmo-Physical Research and Aeronomy SB RAS, Arctic and Antarctic Research Institute, and DMI), and individual magnetic observatories for providing magnetic data used in this study. Work was supported by the RFBR under Grants 14-05-91165 and 15-05-05561.

References

- Akasofu SI (2013) The relationship between the magnetosphere and magnetospheric/auroral substorms. *Ann Geophys* 31 (3):387-394. doi:10.5194/angeo-31-387-2013
- Angelopoulos V, McFadden JP, Larson D, Carlson CW, Mende SB, Frey H, Phan T, Sibeck DG, Glassmeier KH, Auster U, Donovan E, Mann IR, Rae IJ, Russell CT, Runov A, Zhou XZ, Kepko L (2008) Tail reconnection triggering substorm onset. *Science* 321 (5891):931-935. doi:10.1126/science.1160495
- Baker DN, Pulkkinen TI, Angelopoulos V, Baumjohann W, McPherron RL (1996) Neutral line model of substorms: Past results and present view. *J Geophys Res* 101 (A6):12975-13010. doi:10.1029/95ja03753
- Kissinger J, McPherron RL, Hsu TS, Angelopoulos V (2012) Diversion of plasma due to high pressure in the inner magnetosphere during steady magnetospheric convection. *J Geophys Res* 117 (A5):A05206. doi:10.1029/2012ja017579
- Knipp DJ, Emery BA, Richmond AD, Crooker NU, et al. (1993) Ionospheric convection response to slow, strong variations in a northward interplanetary magnetic field: A case study for January 14, 1988. *J Geophys Res* 98 (A11):19273-19292. doi:10.1029/93ja01010
- Laundal KM, Østgaard N (2009) Asymmetric auroral intensities in the Earth's Northern and Southern hemispheres. *Nature* 460 (7254):491-493. doi:10.1038/nature08154
- Lu G, Li WH, Raeder J, Deng Y, Rich F, Ober D, Zhang YL, Paxton L, Ruohoniemi JM, Hairston M, Newell P (2011) Reversed two-cell convection in the Northern and Southern hemispheres during northward interplanetary magnetic field. *J Geophys Res* 116 (A12):A12237. doi:10.1029/2011ja017043
- Lui ATY (1996) Current disruption in the Earth's magnetosphere: Observations and models. *J Geophys Res* 101 (A6):13067-13088. doi:10.1029/96ja00079
- McPherron RL, Russell CT, Aubry MP (1973) Satellite studies of magnetospheric substorms on August 15, 1968: 9. Phenomenological model for substorms. *J Geophys Res* 78 (16):3131-3149. doi:10.1029/JA078i016p03131
- Mishin VV et al (2015a) Positive feedback between ionosphere conductivity and field-aligned current intensity// *Earth Planets Space* (submitted)
- Mishin VV et al (2015b) Versions of model for the solar wind-magnetosphere-ionosphere global electric circuit in substorms of summer and winter seasons// *Earth Planets Space* (submitted)
- Mishin VM et al. (2015c) Field-aligned current dynamics in two selected intervals of the 6 april 2000 superstorm. This issue.
- Østgaard N, Laundal KM, Jussola L, Åsnes A, Håland SE, Weygand JM (2011) Interhemispherical asymmetry of substorm onset locations and the interplanetary magnetic field. *Geophys Res Lett* 38 (8):L08104. doi:10.1029/2011gl046767
- Pellinen RJ, Heikkilä WJ (1978) Energization of Charged Particles to High Energies by an Induced Substorm Electric Field within the Magnetotail. *J Geophys Res* 83 (A4):1544-1550. doi:10.1029/JA083iA04p01544
- Potemra TA (1994) Sources of Large-Scale Birkeland Currents. In: Holtet J, Egeland A (eds) *Physical Signatures of Magnetospheric Boundary Layer Processes*, vol 425. NATO ASI Series. Springer Netherlands, pp 3-27. doi:10.1007/978-94-011-1052-5_1
- Reistad JP, Østgaard N, Laundal KM, Haaland S, Tenfjord P, Snekvik K, Oksavik K, Milan SE (2014) Intensity asymmetries in the dusk sector of the poleward auroral oval due to IMF_{Bx}. *J Geophys Res Space Physics* 119 (12):9497-9507. doi:10.1002/2014ja020216